


# Physical forcing on fish abundance in the southern California Current System

Lia Siegelman-Charbit<sup>1</sup>  | J. Anthony Koslow<sup>2</sup> | Michael G. Jacox<sup>3,4</sup> | Elliott L. Hazen<sup>3</sup> | Steven J. Bograd<sup>3</sup> | Eric F. Miller<sup>5</sup>

<sup>1</sup>Université Pierre et Marie Curie, Paris, France

<sup>2</sup>Scripps Institution of Oceanography, University of California, San Diego, La Jolla, CA, USA

<sup>3</sup>National Oceanic and Atmospheric Administration, Monterey, CA, USA

<sup>4</sup>Institute of Marine Sciences, University of California, Santa Cruz, CA, USA

<sup>5</sup>MBC applied Environmental Sciences, Costa Mesa, CA, USA

## Correspondence

L. Siegelman-Charbit  
Email: lia.siegelman@gmail.com

## Abstract

The California Current System (CCS) is an eastern boundary current system with strong biological productivity largely due to seasonal wind-driven upwelling and transport of the California Current (CC). Two independent, yet complementary time series, CalCOFI ichthyoplankton surveys and sampling of southern California power plant cooling-water intakes, have indicated that an assemblage of predominantly cool-water affinity fishes spanning nearshore to oceanic environments in the southern CCS has declined dramatically from the 1970s to the 2000s. We examined potential oceanographic drivers behind this decline both within and north of the CalCOFI survey area in order to capture upstream processes as well. Empirical orthogonal function (EOF) analyses using output from a data-assimilative regional ocean model revealed significant relationships between the fish time series and spatial patterns of upwelling, upper ocean heat content and eddy kinetic energy in the CCS. Correlation and linear regression analyses indicated that the declining trend in fish abundance was correlated with a suite of factors: reduced offshore and increased inshore upwelling; a long term warming trend combined with more recent interannual variability in ocean temperature; weaker eddy kinetic energy north of Point Conception (35°N), potentially indicating reduced transport of the California Current (CC); increased influence of the California Undercurrent (CUC); and a decline in zooplankton displacement volume across the southern CCS. Understanding how changes in oceanography affect fish populations will offer insights into managing fisheries in a changing climate.

## KEYWORDS

CalCOFI, California Current System, empirical orthogonal function analysis, fish communities, ichthyoplankton, physical oceanography

## 1 | INTRODUCTION

The California Current System (CCS) is the eastern boundary current system associated with the North Pacific Gyre. The CCS is characterized by the offshore southward-flowing California Current, a deep north-flowing California Undercurrent (CUC), seasonal wind-driven upwelling, the coastal winter-time northward-flowing Davidson Current and a recirculation area known as the Southern California Eddy.

Geostrophic flow, Ekman transport, and mesoscale eddy activity all interact to rapidly spread near-surface coastal waters offshore and alongshore, which has considerable implications for primary and secondary production, structure of the pelagic ecosystem and fish production (Checkley & Barth, 2009).

Environmental forcing of the biology of the CCS has been the subject of several multiple studies. Chelton, Bernal, and McGowan (1982) linked zooplankton biomass to equatorward transport of the

California Current (CC), cooler ocean temperatures and large scale climatic forcing such as the El Niño. Changes in winds, stratification, and ocean chemistry are known to impact biological activity across the CCS (Checkley & Barth, 2009; Jacox, Hazen, & Bograd, 2016) and seasonally wind-driven nutrient upwelling has a positive impact on primary and secondary production in the region (Hickey, 1998). Furthermore, Mooers and Robinson (1984) showed that physical patterns such as instabilities, jets, fronts, and eddies, are associated with enhanced biological production across the CCS, and Rykaczewski and Checkley (2008) pointed out that the production of Pacific sardine (*Sardinops sagax*) was positively correlated with offshore wind stress curl in the CCS.

Koslow, Miller, and McGowan (2015) studied the abundance and variability of fish communities in the CCS using principal component (PC) analysis of two complementary long-standing sampling programs for marine fishes off southern California: the California Cooperative Oceanic Fisheries Investigations (CalCOFI), which has sampled fish larvae at 66 standard stations ranging from the 50 m isobath to more than 500 km offshore since 1951 and a power plant environmental monitoring program, which routinely sampled the nearshore fishes entrapped by the power plant cooling-water intakes (PPI) at five sites along the coast of southern California since 1972 (Figure 1). Ichthyoplankton provide a proxy for the relative abundance of adult spawning stocks (Hsieh et al., 2005; Koslow, Goericke, Lara-Lopez, & Watson, 2011; Moser, 1996; Moser, Smith, & Eber, 1987; Moser et al., 2001). Principal component analysis of the CalCOFI ichthyoplankton time series indicated two dominant patterns. PC 1<sub>CalCOFI</sub> captured changes in a number of mesopelagic fishes linked to changing midwater oxygen concentrations (Koslow et al., 2011), whereas PC 2<sub>CalCOFI</sub> captured a pattern exhibited by many of the dominant fish taxa in the region, including six of the seven most abundant in the time series, including Pacific sardine (*S. sagax*), northern anchovy (*Engraulis mordax*), Pacific hake (*Merluccius productus*), and rockfishes (*Sebastes* spp.). Some of the taxa that dominate PC 2<sub>CalCOFI</sub> (e.g., sardine, hake, and rockfishes) are key commercial species, but anchovy is lightly fished (mostly for bait) and other taxa that dominate PC 2<sub>CalCOFI</sub> are not commercially exploited at all, such as abundant mesopelagic fishes, northern lampfish (*Stenobranchius leucopsarus*), and California smooth-tongue (*Leuroglossus stilbius*).

This diverse assemblage, which included epi- and mesopelagic fishes, planktivores and piscivores, is characterized by taxa with cool-water affinities (Koslow et al., 2015; Moser et al., 1987). Many of the fishes that dominated the PPI time series have distributions restricted to the nearshore, such as various small perches (*Phanerodon furcatus*, *hyperprosopon argenteum*, *Cymatogaster aggregate*, and *Embiotoca jacksoni*) and the kelp bass (*Paralabrax clathratus*). Because CalCOFI sampling is predominantly offshore, while the power plant intakes are situated nearshore, most taxa present in the CalCOFI time series were absent from the PPI time series and vice versa, (Table S1). Nevertheless, both PCs exhibited a strong decline from about 1970–2010 and were highly correlated ( $r = .85$ ,  $p < .01$ ), with half of the correlation due to the trend and half to the interannual

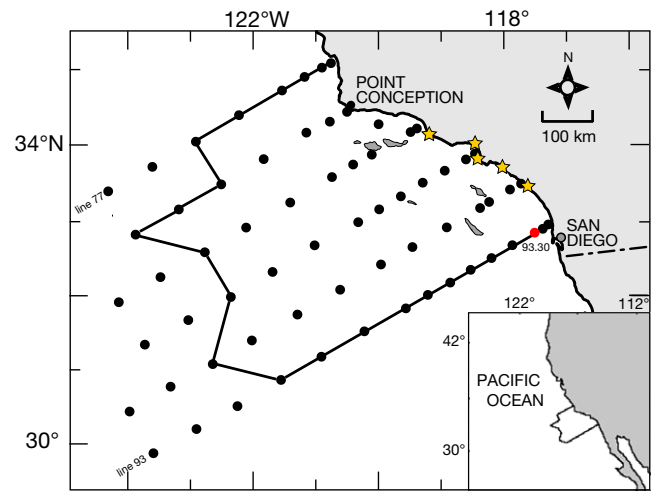


**FIGURE 1** Survey region showing the 66 CalCOFI sampling stations (circles) and the power plant intake (PPI) sites (yellow stars). The red circle shows station 93.30 where spiciness has been measured along the isopycnal  $\sigma_{\theta} = 26.5 \text{ kg/m}^3$ . The solid outline encloses the consistently sampled core stations included in the principal component analysis (PC 2<sub>CalCOFI</sub>)

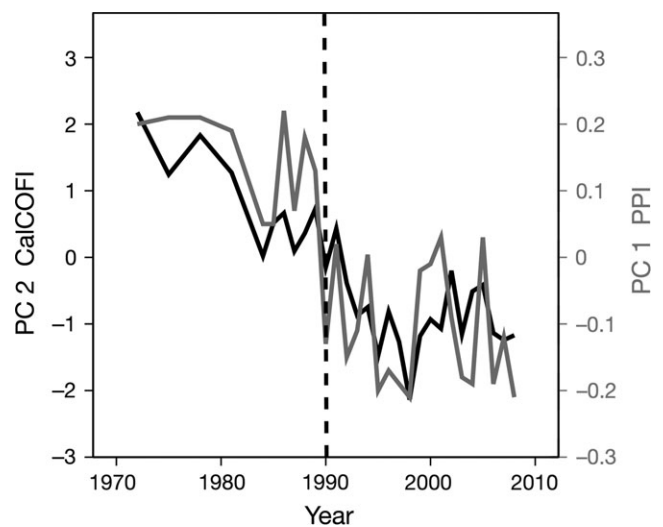


**FIGURE 2** Time series for PC 1<sub>PPI</sub> and PC 2<sub>CalCOFI</sub>. The dashed line indicates an apparent regime shift in 1989–1990, from Koslow et al. (2015)

variability (Figure 2) (Koslow et al., 2015). The abundance of nearshore fishes based on the overall PPI entrapment rate declined 78% from 1972 to 2010 (Miller & McGowan, 2013), while ichthyoplankton taxa that loaded highly on PC 2<sub>CalCOFI</sub> declined 76%. The close congruence between these two time series reflects a strong multi-decadal decline in the dominant fishes of the southern CCS that extends from nearshore to offshore habitats and communities.

It is now widely accepted that climate variability and possibly secular climate change significantly affect marine fish communities (Barry, Baxter, Sagarin, & Gilman, 1995; Hare & Mantua, 2000; Klyashtorin, 1998; Last et al., 2011). The dramatic decline observed by Koslow et al. (2015) across a broad range of fishes in the southern CCS from nearshore to oceanic waters raises the question of the

role of oceanographic drivers, because although several taxa, such as Pacific sardine and Pacific hake, are commercially exploited, many if not most of the taxa that shared this declining trend are not commercially exploited or only lightly fished, including several small mid-water myctophids and bathylagids and small nearshore fishes such as surfperches (embiotocids). Koslow et al. (2015) proposed two hypotheses regarding the decline in fish abundance in the southern CCS: (i) a general warming associated with decreased transport in the CCS leading to a decline in taxa with cool-water affinities, which are generally the most abundant fishes in the region, and (ii) a decline in productivity, also associated with decreased transport in the CCS and associated with a decline in zooplankton (Roemmich & McGowan, 1995), leading to a bottom-up decline in fish abundance. However, the oceanography of the CCS is complex, often displaying differences onshore/offshore and from the northern to southern CCS (Checkley & Barth, 2009), such that even the sign of trends may differ across the region. The use of simple spatially-averaged indices may therefore not be able to adequately represent the signal. This is particularly true for upwelling in the Southern California Bight, the core region sampled by CalCOFI, where simple indices such as the Bakun Index poorly represent vertical velocities at the base of the mixed layer (Bakun, 1973; Jacox, Moore, Edwards, & Fiechter, 2014). Our approach was therefore to use spatially-resolved output from a data-assimilative regional ocean modeling system (ROMS) for the CCS (Neveu et al., 2016). Empirical orthogonal function (EOF) analyses of physical variables, such as upwelling, upper ocean heat content and eddy kinetic energy over the extent of the southern CCS, enabled us to examine how the fish time series were related to spatially resolved patterns of these physical processes. Since many of these variables were inter-related and may exhibit non-linear relationships with fish production, generalized additive models (GAM) and linear models (LM), as well as correlation analyses, were used to assess the relative importance of potential ocean drivers. The use of additional and spatially resolved environmental datasets, together with more rigorous quantitative analyses relating the fish populations to their environment, constitutes a novel and significant contribution to existing literature and represents a significant step forward from past uses of simple indices for transport and upwelling (Koslow et al., 2015) allowing us to look at upstream effects. Our results indicate that several factors, including long-term regional ocean temperature warming until circa 1999, reduced offshore and increased coastal upwelling, as well as decreased eddy kinetic energy indicative of decreased transport north of Point Conception, and suggest that changing ocean conditions are likely responsible for the observed decline in the cool-water marine fish communities off southern California.

## 2 | MATERIALS AND METHODS

### 2.1 | Biological time series

The starting points for our study were the time series described in Koslow et al. (2011), Koslow et al. (2015), Koslow, Davison, Lara-

Lopez, and Ohman (2014), and Miller and McGowan (2013), and the reader is directed there for details of the underlying sampling methodologies and PC analysis.

#### 2.1.1 | CalCOFI ichthyoplankton data

Briefly, we calculated annual mean abundance of larval fish sorted from CalCOFI oblique bongo-net tows from the surface to 210 m depth at 51 consistently sampled core stations (Figure 1). All stations were weighted equally, despite unequal station spacing inshore and offshore, because we looked for relative indices, rather than absolute estimates, of abundance. Larval fish were identified and enumerated to the lowest possible taxon. Taxa were only included in the analysis if present in at least half the years of the time series, such that 86 taxa were included.

#### 2.1.2 | Power plant intake (PPI) data

The PPI data set was derived from periodic sampling of fishes entrapped in the cooling-water intake of five southern California power plants (Figure 1). The intakes ranged from 100 to 960 m offshore and were mostly at about 10 m depth.

The two highly correlated PCs from these data sets (PC 1<sub>PPI</sub> and PC 2<sub>CalCOFI</sub>) ( $r = .85$ ,  $p < .01$ ) reflected fish abundance for nearshore and offshore environments in the southern CCS. Since PC 1<sub>PPI</sub> started in 1972 and PC 2<sub>CalCOFI</sub> had a total of eight missing years between 1972 and 1983, the two PCs were combined into a single PC (PC<sub>fish</sub>) by normalizing and then averaging them, providing a single time series with an enhanced number of degrees of freedom. PC<sub>fish</sub> ranged from 1951 to 2009. Approximately one-third of the high-loading taxa are shared by the two PCs, which contributed to the close correlation between the two time series and enhanced our confidence in interpolating and extrapolating the values of one PC from the other.

#### 2.1.3 | Zooplankton displacement volume (Log Zoo DV)

Mean annual zooplankton displacement volume (DV, units of cm<sup>3</sup>/1,000 m<sup>3</sup>) from the CalCOFI plankton tows after removal of gelatinous zooplankton >5 cm was used as an index of biological productivity and food availability to plankton-feeding fishes. The annual means were log-transformed prior to analysis. The time series ranged from 1951 to 2008.

### 2.2 | Environmental time series

Environmental variables were obtained from the CalCOFI data set as well as a regional ocean model to examine their relationships with observed fish community patterns. Including environmental time series from CalCOFI allowed us to extend the analysis back to 1951 while the regional model output begins in 1980. CalCOFI data included:

### 2.2.1 | Near surface temperature ( $T_{10}$ )

Mean annual temperature at 10 m depth (units of °C), used as a proxy for SST, was obtained from the same stations on the CalCOFI sampling grid from which the ichthyoplankton were obtained. The time series ranged from 1951 to 2008. The CalCOFI near-surface temperature time series is highly correlated with coastal shore temperature time series, such as the Scripps pier time series (Field, Cayan, & Chavez, 2006).

### 2.2.2 | Spiciness

Spiciness is a non-dimensional state variable most sensitive to isopycnal thermohaline variations and least correlated with the density field (Bograd et al., 2015; Flament, 2002). Spiciness is conserved in isentropic motions, and its value increases with increasing temperature and salinity. Spiciness at station 93.30 of the CalCOFI grid (Figure 1) along the isopycnal  $\sigma_{\theta} = 26.5 \text{ kg/m}^3$  was used as a proxy for the influence of the California Undercurrent (CUC, high spiciness indicates strong influence of the CUC, Bograd et al., 2015) and was computed according to Flament (2002). Annual mean temperature, salinity and density were computed as the mean of the cruise values from station 93.30. The time series ranges from 1950 to 2010. The data for salinity and temperature were obtained from the CalCOFI database at <http://www.calcofi.org/data/ctd.html>.

## 2.3 | Ocean model

Spatially explicit estimates of environmental variability were derived from a 31 year (1980–2010) CCS reanalysis using the Regional Ocean Modeling System (ROMS) with four dimensional variational data assimilation. The ROMS model assimilates satellite SSH and SST observations as well as available in situ temperature and salinity data (e.g., CalCOFI surveys, Argo floats) to give a better estimate of the ocean state than either a model or observations alone. The ROMS grid has  $0.1^\circ$  horizontal resolution and uses 42 terrain following coordinates in the vertical, such that the vertical grid resolution that varies from 0.3 to 8 m over the continental shelf and from 7 to 100 m in the deep ocean. It is described in detail by Neveu et al. (2016). Since productivity in the southern CCS is linked to advection of the CC (Chelton et al., 1982) and the local CalCOFI response is likely to be impacted by upstream conditions, we used model output in the southern/central CCS sector ( $30^\circ\text{N}$ – $38^\circ\text{N}$ ,  $116^\circ\text{W}$ – $126^\circ\text{W}$ ) to provide spatially-resolved estimates of upwelling measured by the vertical velocity, heat content, eddy kinetic energy and other potentially relevant variables influencing fish abundance within the CalCOFI domain. At each grid cell, we computed annual means for each variable, with the exception of upwelling for which we used the April–September mean in order to capture the main upwelling season (Huyer, 1983) and its associated strong vertical velocities.

### 2.3.1 | Eddy kinetic energy (EKE)

Eddy Kinetic Energy (units of Joules, J) reflects the strength of the California Current and strong EKE indicates strong transport and mixing within the CCS (Davis & Di Lorenzo, 2015). When stronger alongshore transport interacts with the topography, the result is increased coastal jets, filaments, and eddy activity. Thus, EKE can serve as a proxy for alongshore transport in the California Current, while upwelling drives cross-shore transport. EKE is derived from meridional and zonal components of the surface geostrophic velocity according to  $u_g = \frac{-g}{f} \frac{\partial \eta}{\partial y}$  and  $v_g = \frac{g}{f} \frac{\partial \eta}{\partial x}$  where  $g$  is gravitational acceleration,  $f$  the Coriolis parameter,  $\eta$  the SSH anomaly and  $x$  and  $y$  are oriented eastward and northward, respectively. EKE was then calculated from:

$$\text{EKE} = \frac{u_g^2 + v_g^2}{2}. \quad (1)$$

### 2.3.2 | Upper ocean heat content (H)

Heat content (units of  $\text{J/m}^2$ ) was calculated in the upper 100 m from:

$$H_{100} = \rho c_p \int_{-100}^{\eta} T(z) dz, \quad (2)$$

where  $\rho$  is the density of seawater ( $\sim 1,027 \text{ kg/m}^3$ ),  $c_p$  is the specific heat capacity of seawater ( $\sim 3,990 \text{ J kg}^{-1} \text{ K}^{-1}$ ), and  $T$  is the temperature profile (units of °C).

### 2.3.3 | Vertical velocity (W)

Modeled vertical velocity (m/s) is extracted from ROMS at the base of the mixed layer, with mixed layer depth calculated from the ROMS density field as in Kara, Rochford, and Hurlburt (2000). Positive velocities indicate upwelling while negative velocities indicate downwelling.

## 2.4 | Statistical analyses

### 2.4.1 | Empirical orthogonal function analysis

Empirical orthogonal functions (EOFs) were computed separately for each ROMS variables (EKE, H and W) to study spatial modes of variability and their evolution from 1980 to 2010. For each environmental variable, the temporal variation of the dominant pattern of change, or PC 1, was then used in the correlation and statistical model analyses.

### 2.4.2 | Pearson correlations

Spatial Pearson correlations were computed and mapped between the fish abundance  $\text{PC}_{\text{fish}}$  and the ROMS variables (EKE, H and W).

A data-interpolating variational analysis (DIVA), allowing the spatial interpolation of irregularly spaced data in an optimal way and taking into account topographic and dynamic constraints (Troupin et al., 2012), was subsequently computed between significant correlations ( $p < .05$ ) over the central/southern CCS sector (30°N–38°N, 116°W–126°W). Pearson correlations were also computed between the dominant multivariate pattern of change in fish communities ( $PC_{fish}$ ), the CalCOFI variables ( $T_{10}$ , log-transformed zooplankton DV and spiciness) and the ROMS variables' dominant pattern of change (EKE, H and W PC 1s). Only common years between two time series were kept in the calculations. To assess whether the correlations were based primarily on shared trends among variables and whether they would be observed at interannual time scales as well, correlations were examined before and after detrending. The secular trend was removed from non-stationary variables (variables with significant trend) by extracting the residuals from a linear regression. The correlations were then examined at lags of 0–3 years, since the fish abundance time series reflected the abundance of the spawning stocks (in the case of the CalCOFI ichthyoplankton, Koslow et al., 2011; Moser et al., 2001) and of a combination of juveniles and adults in the case of the PPI time series (Koslow et al., 2015), whereas the environmental influences are presumably strongest during the first year of life when recruitment is determined. In the case of significant autocorrelations, significance levels of results were corrected following Pyper and Peterman (1998) by adjusting the effective number of degrees of freedom ( $N^*$ ):

$$\frac{1}{N^*} = \frac{1}{N} + \frac{2}{N} \sum_{j=1}^{N-1} \rho_{xx}(j) \rho_{yy}(j). \quad (3)$$

where  $N$  is the number of data points in the original time series and  $\rho_{xx}(j)$  and  $\rho_{yy}(j)$  are the autocorrelations of time series  $X$  and  $Y$  at lag  $j$  ( $j$  in years).

### 2.4.3 | Statistical models

Generalized additive models (GAMs) were used to explore linear and non-linear relationships between the environmental variables and fish abundance time series using a Gaussian distribution with the identity link function.  $PC_{fish}$  was used as the response variable and EKE, H and W PC 1s as well as the CalCOFI environmental variables as explanatory variables. Explanatory variables were checked for normality and to ensure low collinearity between explanatory variables, variance inflation factors (VIFs) were kept below 2 (Wood, 2006; Zuur, Ieno, Walker, Saveliev, & Smith, 2009).

Relative contribution of environmental variables to explaining the fish abundance time series was then examined with a linear model (LM). The relative importance of each model predictor was evaluated with four different methods: the LMG (Lindeman, Merenda and Gold) method corresponding to the  $R^2$  contribution averaged over orderings among predictors (Chevan & Sutherland, 1991), the Last method corresponding to each variable contribution when included last, the First method corresponding to each variable contribution

when included first and the Pratt method (Pratt, 1987), which is the product of the standardized coefficient and the correlation. Confidence intervals for relative importance were subsequently bootstrapped. Both GAMs and LMs were selected with a stepwise model selection by exact AIC, which removed the CalCOFI environmental variables from the final models.

Time series averages were calculated with the Matlab software (vR2014b), statistical analyses were performed with the open source R software (v3.2.4), EOFs were conducted using the “prcomp” function in the “stats package”, the GAM analysis was run with the “mgcv package” (v1.8-12; Wood, 2006), the stepwise regression was run using the “stepAIC” function in the “MASS package” and relative importances of the predictors were computed with the “calc.relimp” and “bootval.relimp” functions in the “relaimpo package”. The maps were generated and interpolated with the open source software Ocean Data View (v4.7.1).

## 3 | RESULTS

### 3.1 | Empirical orthogonal function analysis

Empirical orthogonal function analysis was used to objectively identify EKE, H and W's spatial modes of variability and their evolution from 1980 to 2010. The first EOF loadings captured distinct spatial patterns and explained 55.99%, 19.79% and 9.31% of the total variance for H, EKE and W, respectively (Table 1). Jacox et al. (2014) explained 42% of the variance for EOF1 of W based on a similar EOF analysis. However, we normalized the upwelling magnitude in each grid cell prior to running the EOF in order to get the relative pattern of changes in W, while Jacox et al. (2014) used the absolute magnitude of upwelling anomalies in each grid cell. Therefore, variability in the offshore region (where upwelling is relatively weak) accounts for more variance in our analysis, while the nearshore upwelling variability captured by EOF1 accounts for more of the variance in the Jacox et al. analysis. Also, Jacox et al. ran their EOF analysis on monthly data after applying a 12 month running mean, while we ran our EOF analysis on April to September means.

For the EKE, the first PC exhibited a significant decreasing trend from 1980 to 2010 (Figure 3) associated with clear differences between the north and the south of the domain, as well as onshore/offshore in the Southern California Bight (SCB). Positive loadings, corresponding to a decline in EKE, occurred north of Point Conception (35°N) and offshore in the SCB and negative loadings, linked to

**TABLE 1** Percentage of variance explained by the first three eigenvectors for EKE, H and W

	EOF 1	EOF 2	EOF 3
EKE	19.79	8.09	6.24
H	55.99	13.62	4.52
W	9.31	6.18	5.63



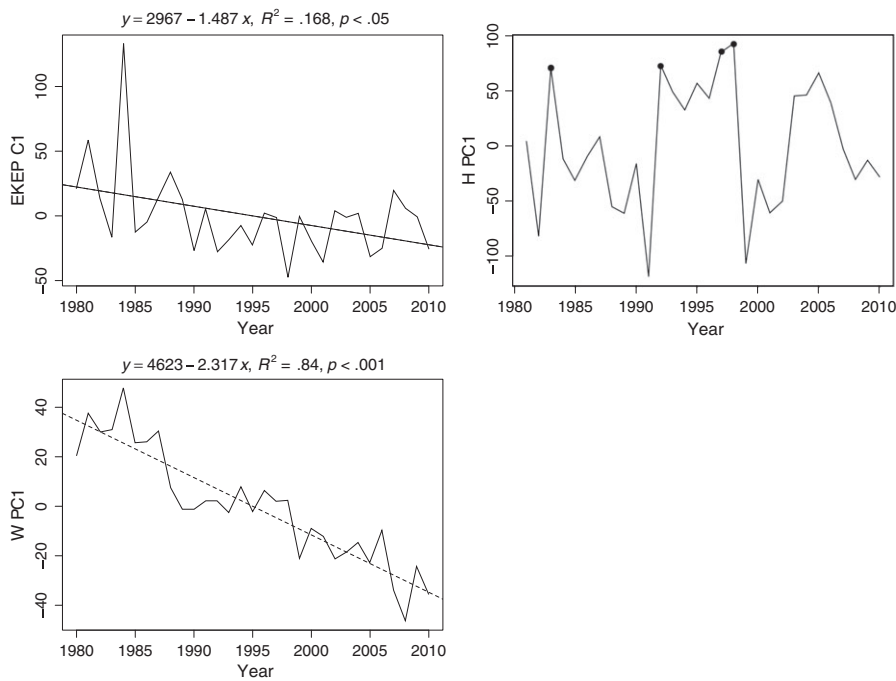


**FIGURE 3** EKE, H and W PC 1 time series from 1980 to 2010 with significant trends in dash. EKE and W exhibit significant decreasing trends while H does not. Black circles indicate strong El Niño years (1983, 1992, 1997 and 1998) apparent in H PC 1

an increase in EKE, were observed south of Point Conception and inshore in the SCB (Figure 4).

For the upper ocean heat content, El Niño years stood out in H PC 1 (Figure 3) and the loadings were strictly positive with an area of weaker loadings nearshore (Figure 4). This indicated an anisotropic spatial pattern where all the grid points contributed in the same direction (but with varying intensity) to H PC 1 time series. The PC data indicated warming from 1980 until 1998, followed by a period of cooling and generally more variable temperatures.

Finally, W PC 1 exhibited a significant decreasing trend from 1980 to 2010 (Figure 3) associated with a distinct spatial pattern between the offshore and nearshore regions: offshore upwelling, characterized by positive loadings, was associated with a decrease in upwelling, while nearshore upwelling loaded negatively along the coast from 30°N to 38°N and was associated with an increase in upwelling (Figure 4; Jacox et al., 2014).

### 3.2 | Pearson correlations

The decline of fishes in the  $PC_{fish}$  time series was significantly spatially correlated with EKE (a proxy for advection and mixing reflecting the strength of the California Current), H (a measure of ocean temperature) and vertical transport W (a measure of upwelling). Spatial correlation maps exhibited significant patterns matching the EOF 1 spatial modes of variability (Figure 5).

For EKE, a clear boundary separating the northern and southern part of the domain was observed; correlations with  $PC_{fish}$  were positive (with a maxima of 0.97) north of Point Conception and in the offshore part of the CalCOFI domain while being negative (with a minima of  $-0.52$ ) inshore and south of 34°N, matching the EKE EOF 1 spatial loadings.

The correlation between  $PC_{fish}$  and H was negative over the entire area (with values  $< -0.2$ ) with a zone of stronger negative correlation parallel to the coast and further offshore as well as north of 36°N. Since  $PC_{fish}$  and H were closely correlated in many areas and no spatial variability was accounted for in  $PC_{fish}$ , the correlations between  $PC_{fish}$  and H showed similar spatial patterns to EOF 1 (H).

Finally, the correlation between  $PC_{fish}$  and W exhibited a distinct spatial pattern, with an area of positive correlation offshore (correlations between 0.2 and 0.98) and a zone of negative correlation nearshore from 30°N to 38°N, which expanded inside the SCB (correlations between 0 and  $-0.81$ ).  $PC_{fish}$  was thus positively correlated with offshore upwelling and negatively correlated with coastal upwelling. Once again, this pattern matched the EOF 1 (W) spatial mode of variability.

Overall, correlation maps highlighted spatial relationships between the fish abundance time series and environmental variables that matched their EOF 1 spatial modes of variability. It also highlighted that, overall, fish abundance was positively linked to offshore upwelling and EKE north of Point Conception and in the major part of the SCB while being negatively linked to coastal upwelling, EKE in the southeastern part of the SCB as well as to temperature in the southern CCS. However, the spatial correlations were not necessarily indicative of biological-environmental correlations, as they also reflected correlations within the environmental fields.

The decline of fishes in the  $PC_{fish}$  time series was significantly correlated with several CalCOFI environmental indicators: mean annual temperature at 10 m from the CalCOFI surveys ( $T_{10}$ ), spiciness along the isopycnal  $\sigma_{\theta} = 26.5 \text{ kg/m}^3$  at station 93.30 of the CalCOFI sampling grid (a proxy for the CUC influence), log-transformed zooplankton displacement volume from the CalCOFI surveys (a proxy for productivity) and PC 1 of EKE, upper ocean heat

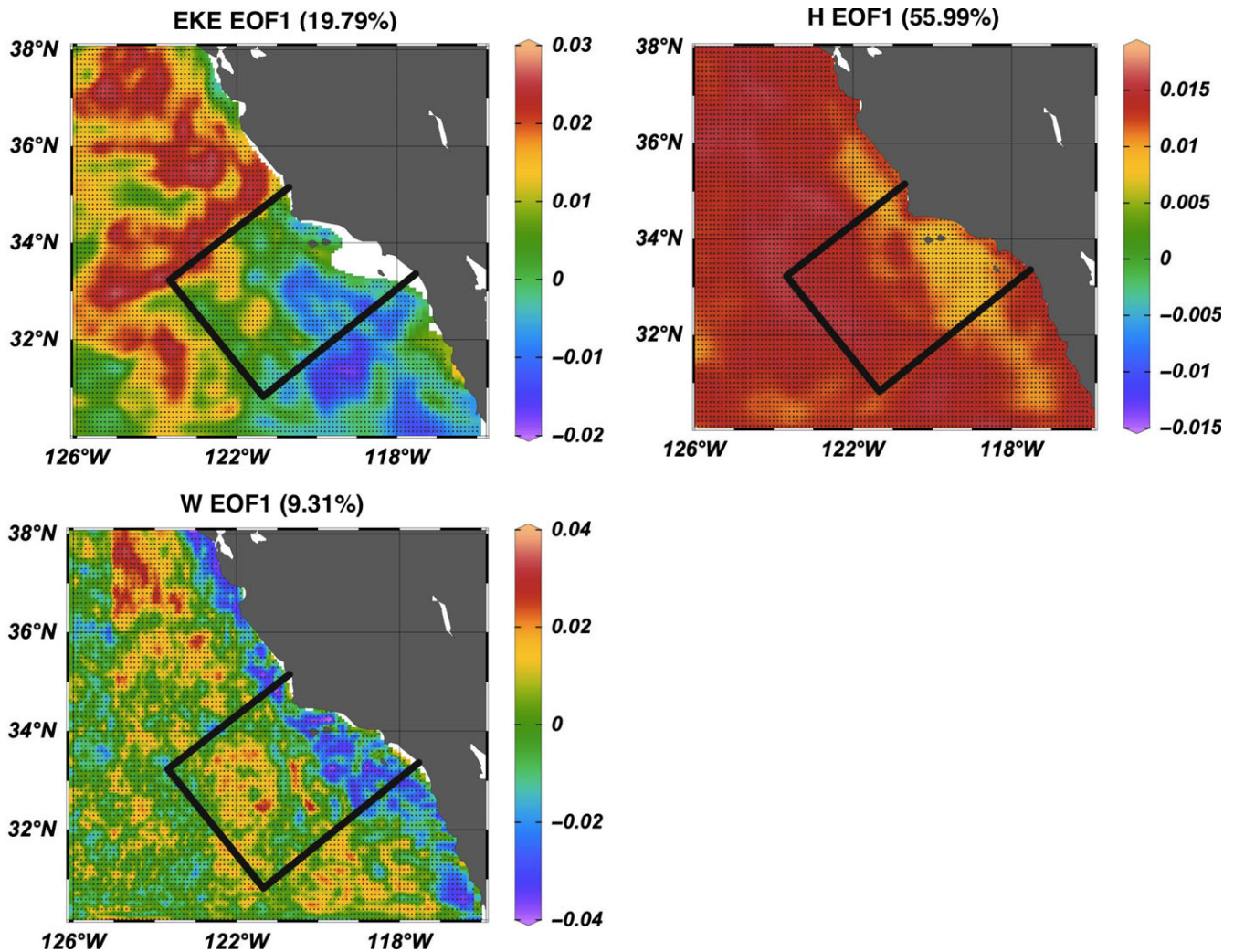


**FIGURE 4** First EOFs loadings map for EKE, H and W with the percentage of the total variance explained by each EOF 1 in parenthesis. Black dots indicate locations of model grid cells. The solid outline corresponds to the CalCOFI study domain and white regions correspond to areas with no model grid cells

content (H) and upwelling (W) (Table 2). The strongest correlations were with the upwelling and log-transformed zooplankton DV ( $r_W = 0.67$ ,  $r_{\log \text{ zoo dv}} = 0.70$ ,  $p < .001$ ). The direction of the correlations were mostly as expected: fish abundance was negatively correlated with  $T_{10}$  and H (cool temperatures were favorable), which was consistent with the positive correlations with W and EKE, indicating that fish abundance was enhanced by increased offshore upwelling in the CCS and advection and mixing north of Point Conception. The negative correlation with spiciness indicated that fish abundance was negatively related to an increased influence of the CUC and its associated tropical warm water flux. The CalCOFI  $T_{10}$  time series indicated an overall warming trend since the 1970s while  $PC_{\text{fish}}$  showed the strongest decline from 1985 to 1998 followed by fluctuations up to 2010 consistent with the H and  $T_{10}$  patterns (Figures 3 and 6). However, surprisingly the decline in fish abundance also appeared to be negatively linked to increased coastal upwelling in the CCS and EKE inside the SCB. After applying a correction for autocorrelation to the effective number of degrees of freedom ( $N^*$ ),

the significance levels were generally reduced but correlations remained significant ( $p < .05$ ) except for EKE and W PC 1, for which the correlations became only marginally significant ( $p < .10$ ) due to their strong significant trends (Table 2).

$T_{10}$ , spiciness, log-transformed zooplankton DV as well as PC 1 for EKE, H and W are inter-correlated variables in the CCS. As expected,  $T_{10}$  and H PC 1 are strongly positively correlated, even after detrending (Table 3). The other noticeable strong intercorrelation is between the log-transformed zooplankton DV and both  $T_{10}$  and H PC 1, as previously noted by Chelton et al. (1982), even after detrending. Spiciness is positively correlated to H PC 1 and negatively correlated to W PC 1, reflecting the fact that tropical waters brought into the region by the CUC are warm. The correlation of fish abundance across the CCS with this set of variables thus suggests that the decline in fish abundance is related to ocean warming, increased coastal upwelling, reduced offshore upwelling and advection as well as an associated decline in productivity and zooplankton prey availability in the CCS (Table 2).

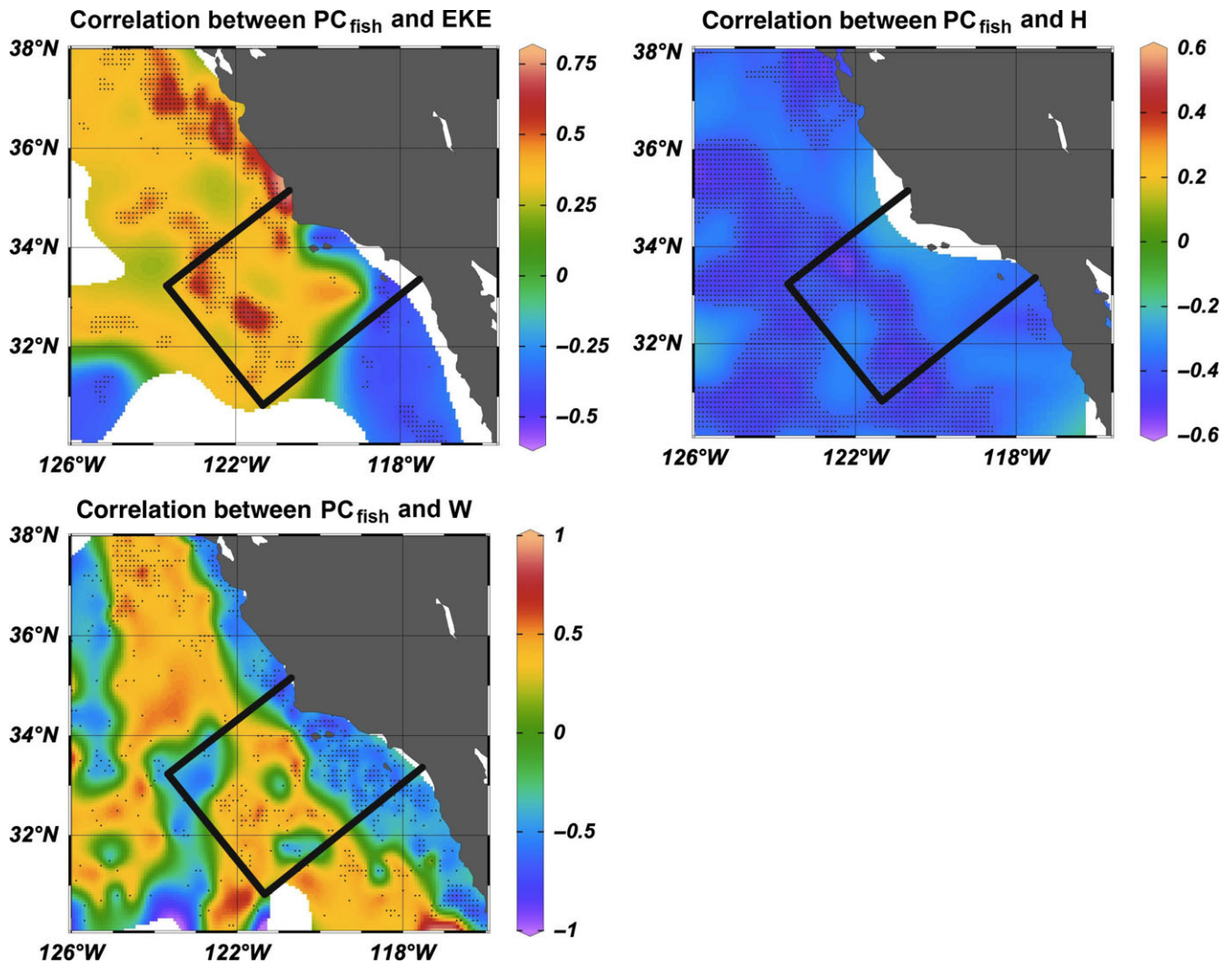


**FIGURE 5** Spatial correlation maps between  $PC_{fish}$  and EKE, H and W. Black dots indicate the presence of significant correlations ( $p < .05$ ). Remaining data points were interpolated with a data-interpolating variational analysis method. The solid outline corresponds to the CalCOFI study domain and white regions correspond to areas with no model grid cells

	$T_{10}$	Spiciness	Log Zoo DV	EKE PC 1	H PC 1	W PC 1
(a) $PC_{fish}$	0.57***	-0.53***	0.70***	0.40*	-0.42*	0.67***
N* and significance	13*	15*	10*	16 <sup>†</sup>	29*	6 <sup>†</sup>
(b) $PC_{fish}$ detrended no lag	-0.34*	-0.44**	0.53***	0.13 <sup>††</sup>	-0.42*	-0.13 <sup>††</sup>
$PC_{fish}$ detrended lag 1 year	0.06 <sup>††</sup>	-0.46***	0.13 <sup>††</sup>	0.13 <sup>††</sup>	-0.03 <sup>††</sup>	0.03 <sup>††</sup>
$PC_{fish}$ detrended lag 2 year	0.04 <sup>††</sup>	-0.58***	0.11 <sup>††</sup>	0.24 <sup>††</sup>	-0.19 <sup>††</sup>	-0.08 <sup>††</sup>
$PC_{fish}$ detrended lag 3 year	0.04 <sup>††</sup>	-0.33*	0.13 <sup>††</sup>	-0.20 <sup>††</sup>	-0.06 <sup>††</sup>	-0.14 <sup>††</sup>

\* $p < .05$ ; \*\* $p < .01$ ; \*\*\* $p < .001$ ; <sup>†</sup> $p < .10$ ; <sup>††</sup> $p > .10$ .

**TABLE 2** Pearson correlations between (a)  $PC_{fish}$  and environmental and biological variables and adjusted degrees of freedom (N\*), (b) detrended PC and detrended environmental and biological variables lagged 0–3 years

However, all these variables, except H, displayed significant trends over the time period: temperature ( $T_{10}$ ) and spiciness increased while EKE PC 1, W PC 1 and log-transformed zooplankton DV decreased

(Figures 3 and 6). This raises the question whether the correlations were based primarily on shared trends among these variables and whether they would also be observed at interannual time scales.



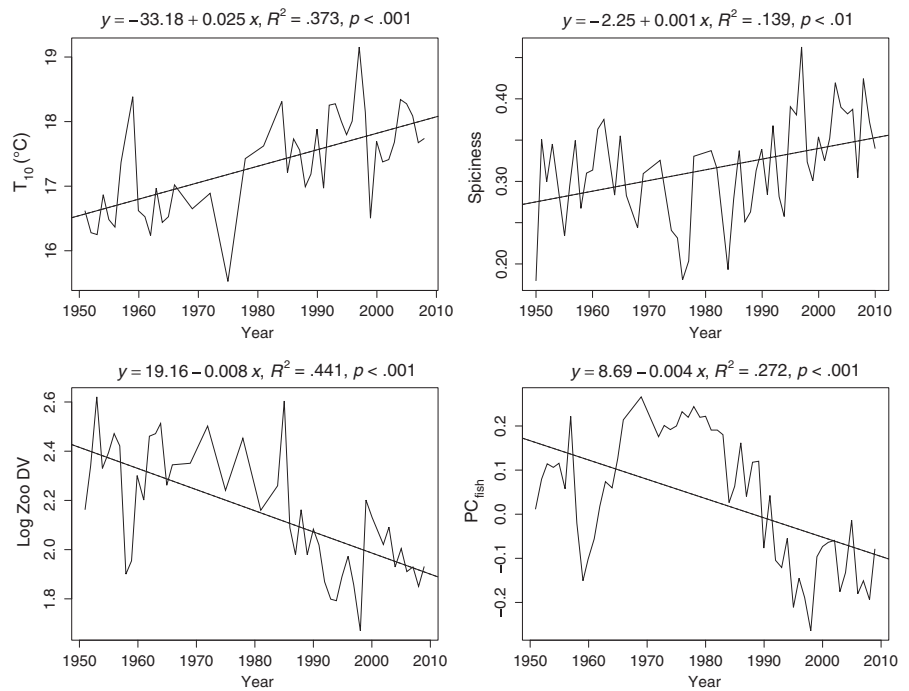


**FIGURE 6** Common trends among environmental variables and fish abundance; mean annual temperature ( $^{\circ}\text{C}$ ) at 10 m from the CalCOFI data set and spiciness at station 93.30 of the CalCOFI grid exhibit significant increasing trends while log-transformed zooplankton DV and  $\text{PC}_{\text{fish}}$  display significant decreasing trends

**TABLE 3** Pearson correlations between (a) environmental and biological variables, (b) detrended environmental and biological variables

		Spiciness	Log Zoo DV	EKE PC 1	H PC 1	W PC 1
(a)	$T_{10}$	0.34***	-0.71***	-0.06 <sup>††</sup>	0.85***	0.07 <sup>††</sup>
	Spiciness		-0.27 <sup>†</sup>	-0.46*	0.42*	-0.52**
	Log Zoo DV			0.37 <sup>†</sup>	-0.52**	0.38*
	EKE PC 1				-0.26 <sup>††</sup>	0.46**
	H PC 1					0.07 <sup>††</sup>
(b)	$T_{10}$	0.18 <sup>††</sup>	-0.51***	0.04 <sup>††</sup>	0.81***	0.53**
	Spiciness		-0.05 <sup>††</sup>	-0.29 <sup>††</sup>	0.38*	-0.10 <sup>††</sup>
	Log Zoo DV			0.23 <sup>††</sup>	-0.52**	0.00 <sup>††</sup>
	EKE PC 1				-0.24 <sup>††</sup>	0.23 <sup>††</sup>
	H PC 1					0.43*

\* $p < .05$ ; \*\* $p < .01$ ; \*\*\* $p < .001$ ; <sup>†</sup> $p < .10$ ; <sup>††</sup> $p > .10$ .

After detrending, the correlations were generally reduced, indicating that some proportion of the relationship was based on shared trend (Table 2). In particular, correlations with detrended EKE and W PC 1 became non-significant, indicating that variation in fish abundance was primarily linked to low frequency change in EKE and upwelling. However, several of the correlations remained significant; in particular, the correlation with H PC 1 was unchanged, indicating that fish abundance time series was related to interannual changes in ocean temperatures. The correlations with spiciness and log-transformed zooplankton DV, and to a lesser extent with  $T_{10}$  remained significant as well. Lagging the environmental variables from 1 to 3 years consistently altered the strength of the relationships with all correlations becoming non-significant, apart from spiciness whose correlations remained significant at all lags. However,  $\text{PC}_{\text{fish}}$  is a composite of many taxa with varying years to recruitment, so it is not

surprising that there was a lack of a peak in the strength of the correlations with varying lags.

### 3.3 | Statistical models

The generalized additive model output showed that H and W PC 1s had significant effects on  $\text{PC}_{\text{fish}}$  while EKE PC 1 did not. The selected model,  $\text{PC}_{\text{fish}} \sim s(W) + s(H) + s(\text{EKE})$ , explained 61.6% of the total variance. The relationships between the fish abundance time series and the environmental variables were linear (Table 4) in the expected direction: negative for H and positive for W (Figure 7).

Since the relationships were all linear, the relative contribution of environmental variables to explaining the PC time series was then examined with a linear model. The results were consistent with the GAM, and only the upwelling index (W PC 1) and the upper ocean

**TABLE 4** GAM summary statistics for best-fit model with variance inflation factors (VIF) below 2 and *df* (degrees of freedom selected by the model) equals to 1 indicating a linear relationship between the explanatory and response variable

	VIF	df	F stat	p	R <sup>2</sup>
EKE PC 1	1.409	0	0.000	.803 <sup>††</sup>	.616
H PC 1	1.127	1	1.585	.001 <sup>***</sup>	
W PC 1	1.317	1	3.774	.000 <sup>***</sup>	

Only upwelling (W PC 1) and upper ocean heat content (H PC 1) had a significant effect on fish abundance, \* $p < .05$ ; \*\* $p < .01$ ; \*\*\* $p < .001$ ; <sup>†</sup> $p < .10$ , <sup>††</sup> $p > .10$ .

heat content (H PC 1) entered the stepwise regression significantly. The selected linear model,  $PC_{fish} \sim W + H$ , explained 64.1% of the total variance (Table 5) with normally distributed and homoscedastic residuals (Table S2). The relative importance of upwelling was striking, with 70% of the  $R^2$  explained by W PC 1 and 30% by H PC 1 (Figure 8). This result was independent of the method and highlights the major role played by upper ocean heat content in relation to long term changes in fish abundance. It suggests an important role for the 31 year trend in W PC1 yet the interannual variability in  $PC_{fish}$  from the early 2000s onwards as well as the biophysical mechanisms that might be involved remain unresolved.

In summary, the statistical models corroborated the Pearson correlations results. Upwelling was consistently the most important factor explaining  $PC_{fish}$  for longer-term trends along with ocean temperature (H for both interannual variability and longer-term trends and  $T_{10}$  for longer-term trends). Our results suggest that fish

**TABLE 5** LM results from stepwise regression analysis

	Estimate	SE	t	p	R <sup>2</sup>
Intercept	-0.045	0.015	-2.924	.007 <sup>**</sup>	.6407
H PC 1	-0.001	0.000	-3.853	.000 <sup>***</sup>	
W PC 1	0.004	0.001	5.770	.000 <sup>***</sup>	

Potential independent variables are:  $T_{10}$ , spiciness, log-transformed zooplankton DV and EKE, H & W PC 1s. \* $p < .05$ ; \*\* $p < .01$ ; \*\*\* $p < .001$ ; Probability to enter is  $p < .05$ . Only the upwelling (W PC 1) and upper ocean heat content (H PC 1) entered the regression significantly.

abundance was negatively impacted by long term warming ocean temperatures, offshore decline and inshore increase in upwelling as well as decreased advection north of Point Conception, increased influence of the CUC and decreased zooplankton displacement volume in the CCS.

## 4 | DISCUSSION

The SCB was chosen as the core CalCOFI sampling region because it is the core region for the spawning of sardine, hake and anchovy. The declines observed in Pacific hake and anchovy in the CalCOFI ichthyoplankton time series are reflected in recent assessments (Grandin et al., 2016; MacCall, Sydeman, Davison, & Thayer, 2016), supporting previous studies that show larval abundance reflects spawning stock biomass (Koslow et al., 2011). However, the SCB is an ecotone where many species with broad cool water (Transition Zone or subarctic) or tropical/subtropical distributions mix, and

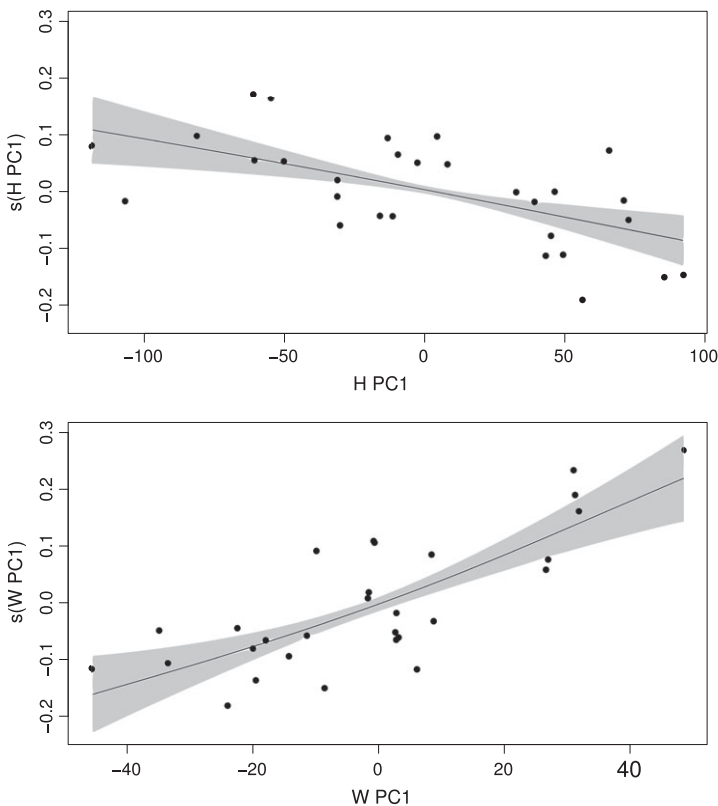


**FIGURE 7** GAM plots showing fish abundance as a function of environmental variables (H and W PC 1s). For each predictor variable, the effect on fish abundance ( $PC_{fish}$ ) is shown on the y-axis and is represented as a spline (s) of the predictor variable. Shaded area represent the 95% confidence interval and the black dots are the partial residuals. The relationships between  $PC_{fish}$  and the environmental variables are linear, negative for H and positive for W

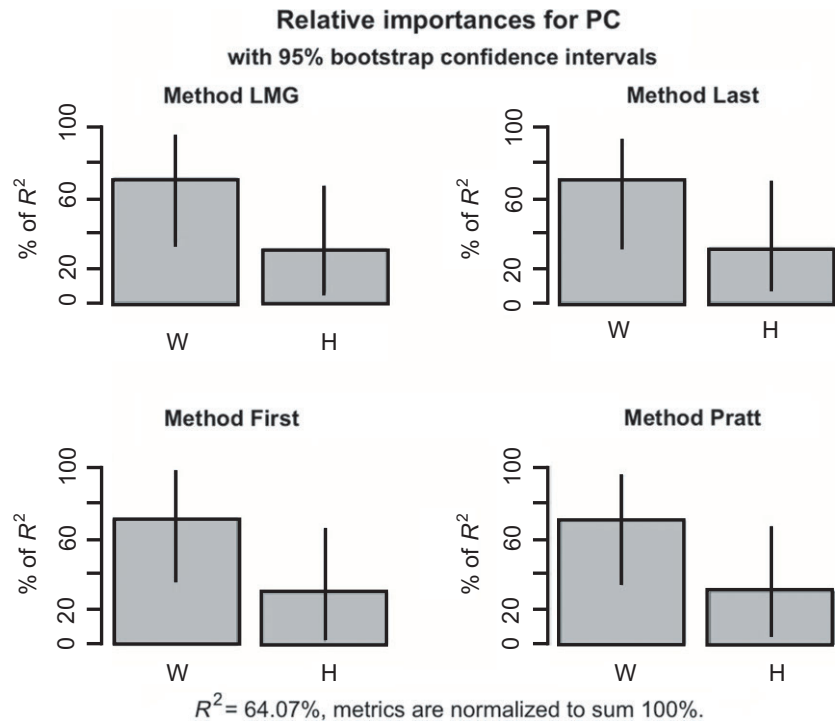


**FIGURE 8** Relative importance of the upwelling (W) and upper ocean heat content (H) variables in explaining the fish abundance time series ( $PC_{fish}$ ) using four different methods; LMG, Last, First and Pratt, all yielding comparable results

changes in fish distribution or the distribution of spawning may also influence larval abundance in the SCB. To test this, ichthyoplankton time series have recently been developed for the region north of Point Conception to  $\sim 37^\circ N$  lat (off San Francisco) based on CalCOFI data obtained in spring, when the cruises are extended to cover the extended distribution of spawning Pacific sardine. Preliminary results indicate the dominant patterns in fish abundance observed in the core CalCOFI domain are highly coherent across this extended portion of the CCS (Davison et al., personal communication, 2016). Furthermore, upstream effects are important and not completely captured by local conditions. For instance, offshore waters in the SCB may have properties characteristic of more northern coastal waters, having been upwelled off central California and subsequently advected to the south.

The broad pattern of decline since ca. 1970 captured in the  $PC_{fish}$  time series includes most of the dominant fishes in the PPI and CalCOFI data sets, including 10 of the 11 most abundant taxa in the CalCOFI time series. Many of these taxa have been identified as a "northern" or cool-water affinity assemblage in the CalCOFI surveys (Koslow et al., 2015; Moser et al., 1987). Their decline is significantly correlated with a broad suite of environmental time series that indicate a 61 year (1950–2010) warming trend in the core CalCOFI domain ( $T_{10}$  and H), reduced advection of the CC (EKE) and increased input of tropical/sub-tropical water into the SCB (spiciness), and a general decline in zooplankton DV (Table 2). The waters north of Pt Conception are markedly higher in nutrient concentration and zooplankton biomass (Reid, 1962), and southward transport of the CC has been shown to be critically linked to the productivity of the CCS, particularly in the Southern California Bight (Chelton et al., 1982). This constellation of relationships therefore suggests that the

decline in cool-water affinity fishes is associated with a decline in the productivity of the southern CCS, linked to declining transport of the CC, as suggested by the trend in EKE.

However, the spatially heterogeneous trends in the ROMS outputs for upwelling (W) off southern California complicate this picture. PC 1 (W) displays a strong declining trend based on an increasing trend in coastal upwelling and a decline in offshore wind-stress curl-driven upwelling (Figure 3). As reviewed by Checkley and Barth (2009), coastal upwelling velocities are an order of magnitude larger than those offshore but occur over a narrower region. The wind-stress curl also contributes significantly to the equatorward transport of the CCS. The declining trend in EKE and offshore wind-stress curl-driven upwelling thus both suggest a decline in the transport of the CC which is consistent with the decline in zooplankton DV, suggestive of an overall decline in productivity of the southern CCS. While there is an increasing trend in upwelling in the SCB, the influence of upwelling on the ecosystem depends not only on upwelling intensity but also on additional factors including stratification, the depth of the nitracline, and nutrient content. Several recent studies concur with the ROMS output, suggesting that coastal upwelling increased between 1980 and 2010 (Di Lorenzo, Miller, Schneider, & McWilliams, 2005; García-Reyes & Largier, 2010; Sydeman et al., 2014), but the nutrient flux depends on stratification and the depth of the nitracline as well as upwelling rate (Jacox, Bograd, Hazen, & Fiechter, 2015). The long-term positive trends in SST (from 1950 to about 2014) and heat flux (H) suggest an increase in stratification, but CalCOFI data from 1984 until about 2014 show no clear trend in nitrate concentration, stratification or nitracline depth in the core CalCOFI domain (McClatchie, Goericke et al., 2016). Trends in chlorophyll from 1997 to 2010 appear mixed in the CCS, with

increasing trends in the central CCS, but declines off Baja California (Kahru, Kudela, Manzano-Sarabia, & Mitchell, 2012). Although no trend in chlorophyll in the core CalCOFI domain is observed in the satellite record from 1997 (Kahru et al., 2012), the CalCOFI cruise record, which extends back to 1984, indicates a slightly increased trend (Wells et al., 2013), at least until the recent warm conditions of 2015–2016.

The coherent decline of a broad suite of the dominant fishes of the CCS thus defies easy explanation. The decline cannot be attributed to fishing: most of the fishes that declined are not commercially fished, including a number of small midwater and nearshore taxa. It is correlated with several oceanographic variables that point to a warming trend (starting from 1950 albeit with decadal-scale reversals) and changes in the transport and water mass characteristics of the CCS (see also Bograd et al., 2015; McClatchie, Thompson et al., 2016). However, evidence for declining productivity is equivocal.

Our findings thus provide limited support for the hypothesis advanced by Koslow et al. (2015) regarding the physical mechanisms behind the decline in fish abundance in the southern CCS. Koslow et al. (2015) pointed out two potential coupled mechanisms: (i) a general warming associated with decreased transport in the CCS leading to a decline in taxa with cool-water affinities, which are generally the most abundant fishes in the region, and (ii) a decline in productivity, also associated with decreased transport in the CCS and associated with a decline in zooplankton (Roemmich & McGowan, 1995), leading to a bottom-up decline in fish abundance. Still, it remains unclear how these factors, which all point to decreased productivity, can be squared with the apparent increasing trend in coastal upwelling. Other potential factors such as top down effects may also explain the variability in larvae abundance; for example, the remarkable increase in the sea lion populations in the CCS region from approximately 50,000 to 340,000 animals from 1975 to 2011 (McClatchie, Field et al., 2016) may have impacted forage fishes, including sardine, anchovy and rockfish in the CalCOFI region. It would therefore be premature to attribute the decline of fishes across the southern CCS to particular environmental mechanisms or to quantitatively assess the roles of climate variability and climate change in driving these changes.

Two recent studies also point to the influence on of warming and advection of warm and cool water masses on the fish community and its diversity in the CCS off southern California (Koslow, McMonagle, & Watson, 2017; McClatchie, Thompson et al., 2016). Both note that despite the strong decline in cool-water CCS endemics (northern anchovy and Pacific hake) and mesopelagic species (*L. stilbius* and *S. leucopsarus*) associated with ocean warming, overall fish community structure in the region appears resilient to date. However, both observed an increase in species richness related to an influx of relatively rare warm-water taxa, which McClatchie, Thompson et al. (2016) related to an increased influx of Pacific Equatorial Water, particularly during the 1997–1998 El Niño, and which Koslow et al. (2017) also observed in relation to the warm phase of the PDO.

For a broader understanding of the drivers behind fish community dynamics on a multi-decadal time scale, the influence of large-scale climatic patterns indexed by variables such as the PDO, MEI and NPGO on the abundance and distribution of fishes in the CCS should be taken into account and is a topic for future investigation. As pointed out by Koslow et al. (2015), the timing of the most marked decline (1989–1990) coincided with a regime shift that has been identified for a range of physical and biological variables along the west coast of North America from the Aleutian Low Pressure Index and SST to a wide range of fishery and other biological time series (Breaker, 2007; Hare & Mantua, 2000). Koslow et al. (2014) also reported that mesopelagic fishes with warm water affinities were positively correlated with SST, sea level at San Francisco (i.e., weak transport of the CCS), the MEI and the PDO.

However, despite these uncertainties, it is clear that fish communities are responding to changing ocean conditions since the early 1970s. Trends of warmer ocean temperature, increased coastal and decreased offshore upwelling, eddy kinetic energy, spiciness, and changes in water mass composition within the CCS, all appear linked to the decline in fish abundance across the southern CCS. The fact that only the long-term trend in some of these variables are significantly related to fish abundance possibly indicates that the controls on fish abundance might be different for interannual timescales versus long-term trends. They also may be related to different processes. For example, EKE and W might relate to the abundance of the population and therefore show up in the trend. In contrast, H might be related to temperature-driven changes in the species distributions (into and out of the CalCOFI grid), and therefore show up in the interannual variability.

This study stresses the importance of a thorough understanding of the physical mechanisms in the southern CCS, especially south of Point Conception, from annual to multi-decadal “regime shift” time scales. This knowledge is essential to understand the drivers influencing fish population dynamics, and to ultimately maintain healthy and well managed ecosystems and fisheries in the North Pacific.

## ORCID

Lia Siegelman-Charbit  <http://orcid.org/0000-0003-3330-082X>

## REFERENCES

- Bakun, A. (1973). *Coastal upwelling indices, west coast of North America*. NOAA Technical Report U.S. Department of Commerce. NMFS SSRF-671, 1946–71, 103 pp.
- Barry, J. P., Baxter, C. H., Sagarin, R. D., & Gilman, S. E. (1995). Climate-related, long-term faunal changes in a California rocky intertidal community. *Science*, 267, 672–675. <https://doi.org/10.1126/science.267.5198.672>
- Bograd, S. J., Buil, M. P., Di Lorenzo, E., Castro, C. G., Schroeder, I. D., Goericke, R., ... Whitney, F. A. (2015). Changes in source waters to the Southern California Bight. *Deep Sea Research Part 2 Topical Studies Oceanography*, 112, 42–52. <https://doi.org/10.1016/j.dsr2.2014.04.009>



- Breaker, L. C. (2007). A closer look at regime shifts based on coastal observations along the eastern boundary of the North Pacific. *Continental Shelf Research*, 27, 2250–2277. <https://doi.org/10.1016/j.csr.2007.05.018>
- Checkley, D. M., & Barth, J. A. (2009). Patterns and processes in the California Current System. *Progress in Oceanography*, 83, 49–64. <https://doi.org/10.1016/j.pocean.2009.07.028>
- Chelton, D. B., Bernal, P., & McGowan, J. A. (1982). Large-scale interannual physical and biological inter-action in the California Current. *Journal of Marine Research*, 40, 1095–1125.
- Chevan, A., & Sutherland, M. (1991). Hierarchical partitioning. *The American Statistician*, 45, 90–96.
- Davis, A., & Di Lorenzo, E. (2015). Interannual forcing mechanisms of California Current transports II: Mesoscale eddies. *Deep Sea Research Part 2 Topical Studies Oceanography*, 112, 31–41. <https://doi.org/10.1016/j.dsr2.2014.02.004>
- Di Lorenzo, E., Miller, A. J., Schneider, N., & McWilliams, J. C. (2005). The warming of the California Current System: Dynamics and ecosystem implications. *Journal of Physical Oceanography*, 35, 336–362. <https://doi.org/10.1175/JPO-2690.1>
- Field, D., Cayan, D., & Chavez, F. (2006). Secular warming in the California Current and North Pacific. *CalCOFI Reports*, 47, 92–108.
- Flament, P. (2002). A state variable for characterizing water masses and their diffusive stability: Spiciness. *Progress in Oceanography*, 54, 493–501. [https://doi.org/10.1016/S0079-6611\(02\)00065-4](https://doi.org/10.1016/S0079-6611(02)00065-4)
- García-Reyes, M., & Largier, J. (2010). Observations of increased wind-driven coastal upwelling off central California. *Journal of Geophysical Research: Oceans*, 115, C04011.
- Grandin, C. J., Hicks, A. C., Berger, A. M., Edwards, A. M., Taylor, N., Taylor, I. G., & Cox, S. (2016). *Status of the Pacific Hake (whiting) stock in U.S. and Canadian waters in 2016* (p. 165). National Marine Fisheries Service and Fisheries and Oceans Canada: Joint Technical Committee of the U.S. and Canada Pacific Hake/Whiting Agreement.
- Hare, S. R., & Mantua, N. J. (2000). Empirical evidence for North Pacific regime shifts in 1977 and 1989. *Progress in Oceanography*, 47, 103–145. [https://doi.org/10.1016/S0079-6611\(00\)00033-1](https://doi.org/10.1016/S0079-6611(00)00033-1)
- Hickey, B. M. (1998). Coastal oceanography of western North America from the tip of Baja California to Vancouver Island. *The Sea*, 11, 345–393.
- Hsieh, C. H., Reiss, C., Watson, W., Allen, M. J., Hunter, J. R., Lea, R. N., ... Sugihara, G. (2005). A comparison of long-term trends and variability in populations of larvae of exploited and unexploited fishes in the Southern California region: A community approach. *Progress in oceanography*, 67, 160–185. <https://doi.org/10.1016/j.pocean.2005.05.002>
- Huyer, A. (1983). Coastal upwelling in the California current system. *Progress in oceanography*, 12, 259–284. [https://doi.org/10.1016/0079-6611\(83\)90010-1](https://doi.org/10.1016/0079-6611(83)90010-1)
- Jacox, M. G., Bograd, S. J., Hazen, E. L., & Fiechter, J. (2015). Sensitivity of the California Current nutrient supply to wind, heat, and remote ocean forcing. *Geophysical Research Letters*, 42, 5950–5957. <https://doi.org/10.1002/2015GL065147>
- Jacox, M. G., Hazen, E. L., & Bograd, S. J. (2016). Optimal environmental conditions and anomalous ecosystem responses: Constraining bottom-up controls of phytoplankton biomass in the California Current System. *Scientific Reports*, 6, 27612. <https://doi.org/10.1038/sre27612>
- Jacox, M., Moore, A., Edwards, C., & Fiechter, J. (2014). Spatially resolved upwelling in the California Current System and its connections to climate variability. *Geophysical Research Letters*, 41, 3189–3196. <https://doi.org/10.1002/2014GL059589>
- Kahru, M., Kudela, R. M., Manzano-Sarabia, M., & Mitchell, G. (2012). Trends in the surface chlorophyll of the California Current: Merging data from multiple ocean color satellites. *Deep Sea Research Part 2 Topical Studies Oceanography*, 77–80, 89–98. <https://doi.org/10.1016/j.dsr2.2012.04.007>
- Kara, A. B., Rochford, P. A., & Hurlburt, H. E. (2000). An optimal definition for ocean mixed layer depth. *Journal of Geophysical Research: Oceans*, 105, 16803–16821. <https://doi.org/10.1029/2000JC900072>
- Klyashtorin, L. B. (1998). Long-term climate change and main commercial fish production in the Atlantic and Pacific. *Fisheries Research*, 37, 115–125. [https://doi.org/10.1016/S0165-7836\(98\)00131-3](https://doi.org/10.1016/S0165-7836(98)00131-3)
- Koslow, J. A., Davison, P., Lara-Lopez, A., & Ohman, M. D. (2014). Epipelagic and mesopelagic fishes in the southern California Current System: Ecological interactions and oceanographic influences on their abundance. *Journal of Marine Systems*, 138, 20–28. <https://doi.org/10.1016/j.jmarsys.2013.09.007>
- Koslow, J. A., Goericke, R., Lara-Lopez, A., & Watson, W. (2011). Impact of declining intermediate-water oxygen on deepwater fishes in the California Current. *Marine Ecology Progress Series*, 436, 207–218. <https://doi.org/10.3354/meps09270>
- Koslow, J. A., McMonagle, H., & Watson, W. (2017). Influence of climate on the biodiversity and community structure of fishes in the southern California Current. *Marine Ecology Progress Series*, 571, 193–206. <https://doi.org/10.3354/meps12095>
- Koslow, J. A., Miller, E. F., & McGowan, J. A. (2015). Dramatic declines in coastal and oceanic fish communities off California. *Marine Ecology Progress Series*, 538, 221–227. <https://doi.org/10.3354/meps11444>
- Last, P. R., White, W. T., Gledhill, D. C., Hobday, A. J., Brown, R., Edgar, G. J., & Pecl, G. (2011). Long-term shifts in abundance and distribution of a temperate fish fauna: A response to climate change and fishing practices. *Global Ecology and Biogeography*, 20, 58–72. <https://doi.org/10.1111/j.1466-8238.2010.00575.x>
- MacCall, A. D., Sydeman, W. J., Davison, P. C., & Thayer, J. A. (2016). Recent collapse of northern anchovy biomass off California. *Fisheries Research*, 175, 87–94. <https://doi.org/10.1016/j.fishres.2015.11.013>
- McClatchie, S., Field, J., Thompson, A. R., Gerrodette, T., Lowry, M., Fiedler, P. C., ... Vetter, R. D. (2016). Food limitation of sea lion pups and the decline of forage off central and southern California. *Royal Society Open Science*, 3(3), 150628. <https://doi.org/10.1098/rsos.150628>
- McClatchie, S., Goericke, R., Leising, A., Auth, T. D., Bjorkstedt, E., Robertson, R. R., ... Chavez, F. P. (2016). State of the California Current 2015-16: Comparisons with the 1997-98 El Niño. *CalCOFI Reports*, 57, 57.
- McClatchie, S., Thompson, A. R., Alin, S. R., Siedlecki, S., Watson, W., & Bograd, S. J. (2016). The influence of Pacific Equatorial Water on fish diversity in the southern California Current System. *Journal of Geophysical Research*, 121, 6121–6136.
- Miller, E. F., & McGowan, J. A. (2013). Faunal shift in Southern California's coastal fishes: A new assemblage and trophic structure takes hold. *Estuarine, Coastal and Shelf Science*, 127, 29–36. <https://doi.org/10.1016/j.ecss.2013.04.014>
- Moers, C. N., & Robinson, A. R. (1984). Turbulent jets and eddies in the California Current and inferred cross-shore transports. *Science*, 223, 51–53. <https://doi.org/10.1126/science.223.4631.51>
- Moser, H. (1996). The early stages of fishes in the California Current region. *CalCOFI Atlas*, 33, 1505.
- Moser, H. G., Charter, R. L., Watson, W., Ambrose, D. A., Hill, K. T., Smith, P. E., ... Charter, S. R. (2001). The calcofi ichthyoplankton time series: Potential contributions to the management of rocky-shore fishes. *California Cooperative Oceanic Fisheries Investigations Report*, 42, 112–128.
- Moser, H. G., Smith, P. E., & Eber, L. E. (1987). Larval fish assemblages in the California Current region, 1954–1960, a period of dynamic environmental change. *California Cooperative Oceanic Fisheries Investigations Report*, 28, 97–127.
- Neveu, E., Moore, A. M., Edwards, C. A., Fiechter, J., Drake, P., Crawford, W. J., ... Nuss, E. (2016). An historical analysis of the California

- Current circulation using ROMS 4d-var. Part I: System configuration and diagnostics. *Ocean Modelling*, 99, 133–151. <https://doi.org/10.1016/j.ocemod.2015.11.012>
- Pratt, J. W. (1987). Dividing the Indivisible: Using simple symmetry to partition variance explained. *Proceedings of Second Tampere Conference in Statistics*. 245–260.
- Pyper, B. J., & Peterman, R. M. (1998). Comparison of methods to account for autocorrelation in correlation analyses of fish data. *Canadian Journal of Fisheries and Aquatic Sciences*, 55, 2127–2140. <https://doi.org/10.1139/f98-104>
- Reid, J. L. J. (1962). On circulation, phosphate-phosphorus content, and zooplankton volumes in the upper part of the Pacific Ocean. *Limnology and Oceanography*, 7, 287–306. <https://doi.org/10.4319/lo.1962.7.3.0287>
- Roemmich, D., & McGowan, J. (1995). Climatic warming and the decline of zooplankton in the California Current. *Science*, 267, 1324. <https://doi.org/10.1126/science.267.5202.1324>
- Rykaczewski, R. R., & Checkley, D. M. (2008). Influence of ocean winds on the pelagic ecosystem in upwelling regions. *Proceedings of the National Academy of Sciences USA*, 105, 1965–1970. <https://doi.org/10.1073/pnas.0711777105>
- Sydeman, W., García-Reyes, M., Schoeman, D., Rykaczewski, R., Thompson, S., Black, B., & Bograd, S. (2014). Climate change and wind intensification in coastal upwelling ecosystems. *Science*, 345, 77–80. <https://doi.org/10.1126/science.1251635>
- Troupin, C., Barth, A., Sirjacobs, D., Ouberdous, M., Brankart, J. M., Bras-seur, P., ... Lenartz, F. (2012). Generation of analysis and consistent error fields using the Data Interpolating Variational Analysis (DIVA). *Ocean Modelling*, 52, 90–101. <https://doi.org/10.1016/j.ocemod.2012.05.002>
- Wells, B., Schroeder, I. D., Santora, J. A., Hazen, E. L., Bograd, S. J., Bjorkstedt, E. P., & Thompson, A. R. (2013). State of the California Current 2012-13: No such thing as an “Average” Year. *CalCOFI Reports*, 54, 37–71, Fig 14A.
- Wood, S. (2006). *Generalized additive models: An introduction with R*. Boca Raton, FL: CRC Press.
- Zuur, A., Ieno, E., Walker, N., Saveliev, A., & Smith, G. (2009). *Mixed effects models and extensions in ecology with R*. New York, NY: Springer. <https://doi.org/10.1007/978-0-387-87458-6>

## SUPPORTING INFORMATION

Additional supporting information may be found online in the Supporting Information section at the end of the article.

**How to cite this article:** Siegelman-Charbit L, Koslow JA, Jacox M, Hazen E, Bograd S, Miller EF. Physical forcing on fish abundance in the southern California Current System. *Fish Oceanogr*. 2018;27:475–488. <https://doi.org/10.1111/fog.12267>